Progress in Biomaterials (2020) 9:139–151
https://doi.org/10.1007/s40204-020-00138-z

ORIGINAL RESEARCH

Artemisia annua L. as a promising medicinal plant for powerful wound healing applications

Fatemeh Sadat Mirbehbahani[1] · Fatemeh Hejazi[2] · Najmeh Najmoddin[1] · Azadeh Asefnejad[1]

Received: 2 August 2020 / Accepted: 19 September 2020 / Published online: 28 September 2020

Abstract

Artemisia annua L. has been utilized for the first time in a nanofibrous wound dressing composition. The extract of this valuable plant provides anti-inflammatory, anti-bacterial and anti-microbial properties which can be considered as a promising medicinal component in therapeutic applications. In the present work, *Artemisia annua* L. was picked up from Gorgan forest area of Northern Iran and its extract was prepared by methanol as the extraction solvent. In the fabrication of wound dressing, *Artemisia annua* L. extract was mixed with gelatin and a nanofibrous structure was formed by electrospinning technique. To have a wound dressing with acceptable stability and optimum mechanical properties, this biologically active layer was formed on a PCL nanofibrous base layer. The fabricated double-layer wound dressing was analyzed chemically, structurally, mechanically and biologically. ATR-FTIR spectra of the prepared wound dressing contain functional groups of *Artemisia annua* L. as peroxide groups, etc. SEM micrographs of electrospun gelatin/*Artemisia annua* L. confirmed the successful electrospinning process for producing *Artemisia annua* L.-containing nanofibers with mean diameter of 242.00 ± 67.53 nm. In vitro *Artemisia annua* L. release study of the fabricated wound dressings suggests a sustain release over 7 days for the crosslinked sample. In addition, evaluation of the in vitro structural stability of the prepared wound dressings confirmed the stability of the crosslinked nanofibrous structures in PBS solution environment. Biological study of the *Artemisia annua* L.-containing wound dressing revealed no cytotoxicity, good proliferation and attachment of the seeded fibroblasts cells and acceptable antibacterial property against *Staphylococcus aureus* bacteria.

Keywords *Artemisia annua* L. · Wound dressing · Electrospinning · Antibacterial property · Gelatin–*Artemisia annua* L. nanofibers

Introduction

Skin as the largest organ of human body serves as the barrier, which protects inner organs from microbial invasion and UV radiation. This organ with about 2 m^2 area regulates the temperature of the body as well as assisting immune system and sensory detection process of the body (Singer and Clark 1999; Böttcher-Haberzeth et al. 2010). However, skin injuries happen very often and may lead to severe bleeding and sometimes are life threatening. Wounds, the skin injuries, are described as defects in the skin due to mechanical/thermo-damages and other accidents (Rezvani Ghomi et al. 2019). The skin repair process corresponds to restoring the structure and function of skin ECM, which is usually comprised of four steps: inflammation, migratory, new tissue formation, and tissue remodeling. The inflammation phase is the most critical stage, protecting wounds from invading bacteria and assisting the tissue repair process (Liu and Jia 2018). Accordingly, most wound dressings target and facilitate the inflammation stage, support the wound bed and protect it from the factors that may delay or impede its healing such as contaminations and moisture loss and mimic the structure and functions of skin ECM (Naseri-Nosar and Ziora. 2018). In the past, natural materials such as honey and herbal plants were used as wound dressing. Nowadays, wound dressings include natural and synthetic polymers, as well as their combinations with herbal plants (Okur et al.

✉ Fatemeh Hejazi
f.hejazi@shirazu.ac.ir

✉ Najmeh Najmoddin
najmoddin@srbiau.ac.ir

[1] Department of Biomedical Engineering, Science and Research Branch, Islamic Azad University, Tehran, Iran

[2] Department of Advanced Technologies, Shiraz University, Shiraz, Iran

2020; Belachew et al. 2020; Krishnan and Thomas 2019), nanomaterials, etc., in various forms such as films, sponges and hydrogels are designed to facilitate wound healing with improved quality (Stoica et al. 2020).

Medicinal plants attract the attention of researchers worldwide as potential sources of natural compounds with biological activities. Traditional medicinal plant remedies have been highlighted as alternative medicines that are less likely to cause adverse side effects, unlike synthetically generated chemical substances (Kim et al. 2015). *Artemisia annua* L. is an annual herb native to Asia and other continents, and has been used for the treatment and prevention of fever, chills and malaria, in traditional and modern medicine (Hien and white 1993). Detailed analyses such as gas chromatography (GC–MS) have been done to characterize *Artemisia annua* L. The natural products found in *Artemisia annua* L. can be categorized into eight broad groups, including (1) monoterpenes; (2) sesquiterpenes; (3) diterpenes, (4) sterols and triterpenes; (5) aliphatic hydrocarbons, alcohols, aldehydes and acids; (6) aromatic alcohols, ketones and acids; (7) phenylpropanoids; and (8) flavonoids (Brown, 2010; Czechowski et al. 2018). GC–MS analysis has been widely used to characterize *Artemisia annua* L. and it has been revealed that its extract contains a number of valuable compounds (Verdian-rizi et al. 2008; Anshul et al. 2013; Bhakuni et al. 2001). Majority of known GC–MS-detected compounds of *Artemisia annua* L. extracts are monoterpenes and sesquiterpenes. Several major monoterpenes are Artemisia ketone, camphor, camphene, borneol, a-pinene, and 1,8-cineole together with some minor monoterpenes such as α-myrcene, α-terpinene, chrysanthenone and α-copaene; sesquiterpenes are velleral, sabinene and cissabinene hydrate and germacrene A. Isofraxidin is another component of *Artemisia annua* L. which is a coumarin with anti-inflammatory and anti-tumor activities. Artemisia ketone has revealed antifungal activities and a velleral, a sesquiterpene dialdehyde compound has shown antibacterial activities. Germacrene A is a sesquiterpene common across the Asteraceae family for which it has been demonstrated that its downstream metabolism parallels artemisinic acid biosynthetic pathway (Niu et al. 2012; Yamazaki and Tokiwa 2010; Santomauro et al. 2016; Anke and Sterner 1991; Nguyen et al. 2010). Artemisinin is one of the main components of *Artemisia annua* L. extract which contains a peroxide bridge (C–O–O–C) in its formula ($C_{15}H_{22}O_{15}$). Artemisinin has been widely used for the treatment of malaria for the past 2 decades (De vries and Dien 1996). Additionally, artemisinin is known to have antibacterial, antifungal, antiinfection, antileishmanial, antioxidant, antitumor, and anti-inflammatory activities (Cavar et al. 2012; Donata et al. 2015). The extent of the given components relates to the plant origin, plant age (juvenile, mature or old), and the method and solvent of extraction (Czechowski et al. 2018; Kim et al. 2015).

Owing to its unique properties (such as antibacterial, antimicrobial, anti-inflammatory and antiinfection properties) *Artemisia annua* L. is considered as a promising component to be used in wound healing applications. In addition to the mentioned applications (treatment of malaria and etc.), in few studies, *Artemisia* species have been used in wound healing application because of their antibacterial, anti-microbial and anti-inflammatory properties (Derda et al. 2016; Ranjbar and Yousefi 2018; Kaboutari Katadj et al. 2016). As far as our knowledge based on the mentioned studies is concerned, this plant extract application has not been reported yet on wound sites in the form of topical paste or ointment and fabrication of wound dressing composed of *Artemisia annua* L. with nanofibrous structure.

In this work, *Artemisia annua* L. plant was picked up from Northern region of Iran and its methanol extract was prepared. The obtained extract was used for the fabrication of a novel wound dressing. Gelatin–*Artemisia annua* L. extract nanofibers were successfully prepared by electrospinning technique for the first time and collected on the PCL nanofibrous layer. To produce nanofibers, gelatin containing *Artemisia annua* L. extract was used; 1,1,1,3,3,3-hexafluoro-2-propanol (HFIP) was used as the solvent to prepare the electrospinning solution. This alcohol-based solvent is a proper solvent for both gelatin and *Artemisia annua* L. extract and would have minimum effect on the biological properties of this plant extract. Structural, physical and mechanical analyses were performed on the obtained samples. To evaluate the biological properties of the fabricated wound dressing, cytotoxicity and cytocompatibility tests were done using L929 fibroblast cells and antibacterial test was performed by *Staphylococcus aureus* bacteria.

Materials and methods

Materials

Polycaprolactone (PCL), MW 80,000 Da, and gelatin (type A) were purchase from Sigma-Aldrich, USA. Acetic acid (CH_3COOH, 100%), formic acid (HCO_2H, > 98%), methanol (CH_3OH, 80%), glutaraldehyde (2.5%) and hexafluoroisopropanol (HFIP) were purchased from Merck, Germany. Dimethyl sulfoxide solution, Mueller–Hinton agar, trypsin, phosphate-buffered saline (PBS), and 3-[4,5-dimethylthiazol-2-yl]-2,5-diphenyltetrazolium bromide (MTT) were purchased from Sigma-Aldrich, USA. DMEM/F12, and fetal bovine serum (FBS) were provided by Gibco®, USA. *Staphylococcus aureus* (ATCC 25923) was obtained from PadtanTeb Company, Iran. L929 fibroblast cells were purchased from Pasteur institute of Iran, cell bank. *Artemisia annua* L. was collected from Khazar region of Iran, nearby Gorgan Province in Alang dareh forest area.

Extraction of *Artemisia annua* L. plant

The collected plants were dried at 25 °C in the shade for about 96 h and powdered afterwards. One gram of the obtained powder was dissolved in 10 mL ethanol solution (80% (v/v)) in a sealed container and stirred for 24 h. The content was then filtered using filter paper and centrifuged at 10,000 rpm for 30 min in 2 °C. The obtained extract was then freeze dried at − 80 °C for 7 h and stored at − 30 °C for further use. The process of plant extraction is summarized in Fig. 1.

Polymer solution preparation

The PCL solution (17% by w/v) was prepared in solvent system consisting of acetic acid/formic acid in 1:9 ratio and dissolved at 50 °C under constant stirring (1000 rpm) for 8 h (Hejazi and Mirzadeh 2016). Moreover, the solution of gelatin in HFIP (10% by w/v) was prepared at 40 °C under constant stirring (1000 rpm) for 8 h. To obtain gelatin solution, the *Artemisia annua* L. extract was dissolved in HFIP (9% by w/v) at 40 °C under constant stirring (1000 rpm) for 8 h and 2 h prior to electrospinning, the prepared extract was added into the prepared gelatin solution in HFIP, with *Artemisia annua* L. to gelatin weight ratio of 1:4–5.

Electrospinning process

The prepared PCL solution was taken in a 5-mL syringe and loaded in the electrospinning setup (Fanavaran nanomeghyas, Iran). Electrospinning was performed with an applied voltage of 18 kV, flow rate of 0.8 mL/h and the needle tip to collector distance (air gap) of 12 cm for 3 h. To increase the distance between the collected nanofibers and subsequent enhancement of oxygen permeability of the fabricated wound dressing, the rotating mandrel (300 rpm) was covered with a piece of metal mesh No. 10 and electrospinning was done towards this modified collector. As a control for examining the morphology, PCL nanofibers were also collected on the conventional rotating mandrel (300 rpm, without the covered metal mesh).

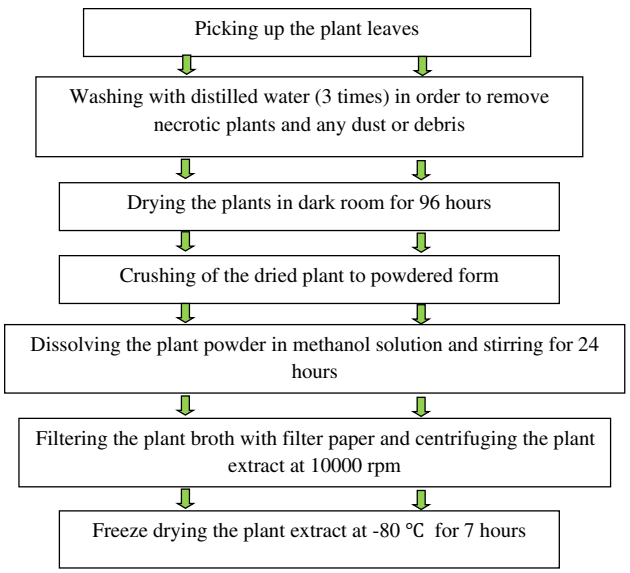

Fig. 1 Extraction process of *Artemisia annua* L.

In the next step, the prepared gelatin or gelatin–*Artemisia annua* L. solution was electrospun on the prepared PCL mat with an applied voltage of 14 kV, flow rate of 0.7 mL/h and the needle tip to collector distance (air gap) of 15 cm for 2 h. The fabricated samples were named as PCL/gelatin (PG), PCL/gelatin–*Artemisia annua* L. (PGA). The fabricated samples were crosslinked by exposure to glutaraldehyde solution (2.5%) vapor for 5 h at room temperature. Samples were then rinsed with distilled water six times and named as crosslinked PCL/gelatin–*Artemisia annua* L. (PGA-x).

FTIR and ATR-FTIR analysis

Artemisia annua L. extract was analyzed by FTIR spectroscopy (BOMEM MB-SRG 1100 G, Canada). Furthermore, the fabricated nanofibrous samples (including the samples containing *Artemisia annua* L. extract) were also analyzed by ATR-FTIR spectroscopy (BOMEM MB-SRG 1100 G, Canada). The tests were performed over infrared range of 400–4000 cm^{-1}, at the resolution of 2 cm^{-1} and 20 scans.

SEM observations

The morphology of the electrospun fibers was analyzed using a scanning electron microscope (SERON/TECHNOLOGY (ALS 2100), South Korea) at an accelerating voltage of 17–20 kV, after sputter coating with gold. Image analysis software (Image J™, NIH, MD, USA) was applied for determining the average diameter of fibers. For this aim, 25 fibers in each SEM image were considered and their diameters were measured. Average diameters are expressed as mean value ± standard deviation. To evaluate the fiber diameter uniformity, diameter distribution histograms are provided based on the measured diameters.

Artemisia annua L. release study

To determine the UV–Vis absorbance of *Artemisia annua* L., the prepared extract was analyzed using UV–Vis spectrophotometer (UNICO, USA) at wavelength (λ) between 200 and 800 nm. Afterwards, *Artemisia annua* L., released from the fabricated samples, was assessed by following the extent of UV–Vis absorbance peaks of *Artemisia annua* L. in the sample's extracts. To prepare the extracts, PCL/gelatin (PG),

PCL/gelatin–*Artemisia annua* L. (PGA) and the crosslinked PCL/gelatin–*Artemisia annua* L. (PGA-x) samples were cut in 1×1 cm^2 cubic specimens, weighed accurately and incubated in 10 mL PBS solution at 37 °C in shaker incubator. To avoid the dissolution rate to be affected by increasing the concentration of the releasing components over the test period, saturation concentration of the gelatin–*Artemisia annua* L. mixture (with the same ratio as in the fabrication process) in PBS was determined and the dimension of samples and volume of incubating media were fixed so that the overall concentration of releasing components over the test duration became at most 30% of the obtained saturation concentration.

At specific time points (1, 3, 5 and 7 days), specimens were removed from the incubation solution. Then the UV–Vis absorbance of each solution was evaluated at wavelength range of 200–800 nm. In all the measurements, PBS solution was considered as control.

Morphological stability

To make an assessment of morphological stability, samples (PG, PGA and PGA-x) were cut into pieces of 1×1 cm^2, precisely weighed (W_0) and then immersed in PBS solution in a continuous shaking water bath with speed of 80 rpm at 37 °C. At predetermined periods of soaking time (1 and 3 days), three paralleled specimens of each type of samples were taken out, and after vacuum drying, were studied by SEM.

Mechanical properties

Mechanical properties of the electrospun wound dressings were analyzed by Tensile Testing Machine (Tinius Olsen H1KS, SDL ATLAS, USA), at a crosshead rate of 10 mm/min and applying 1 kN load cell in dry condition. Specimens with average dimensions of 0.5 cm × 5 cm were prepared and mounted between two grips. The resulting load/deformation curves were converted into stress/strain curves. Young's modulus (E) was calculated as change in stress divided by change in strain in the linear portion of the curve. Tensile strength and elongation-at-break was obtained from the ultimate stress and strain-at-failure, respectively. Tensile test was repeated 5 times on each sample and the average value of E (MPa) and strain-at-break (%) were reported.

In vitro cytotoxicity evaluation

The cell viability and proliferation on the nanofibrous scaffolds were determined using the colorimetric MTT assay. The electrospun samples (PG and PGA-x) were placed in a 96-well cell culture plate. These nanofibrous mats were sterilized under ultraviolet (UV) light for 20 min and washed with PBS. L929 fibroblast cell line was maintained in Dulbecco's Modified Eagle Medium (DMEM) with 10% fetal bovine serum (FBS) at 37 °C in a humidified atmosphere with 5% CO_2 incubator (BINDER, Germany). Afterwards, the fibroblast cells (10,000 cell/200 µL) were seeded on the samples and incubated for cell growth. The culture medium was changed every 3–4 days.

For the MTT assay, samples were rinsed with PBS to remove unattached cells and incubated with 500 µL MTT reagent (0.5 mg/mL stock in PBS) for a period of 5 h at 37 °C. The medium was discarded completely and isopropanol was added to the wells to dissolve the formant crystals. After that, the number of viable cells was recorded at three different time points (1, 3 and 7 days). Fresh culture medium was used as a control. The absorbance was measured at 570 nm using a microplate reader (ELISA reader, STAT FAX 2100, USA). The relative cell viability (compared to control) was calculated as follows:

$$\text{Relative cell viability } (\%) = (\text{OD}_s/\text{OD}_c \times 100),$$

where OD_s and OD_c represent optical density of sample and control, respectively.

Cell morphological observation

The cell morphology and distribution on the scaffolds were observed by SEM. After 1, 3 and 7 days of culture with cells, the scaffolds were washed with PBS and then 50 µL of glutaraldehyde (2.5%) was added into every well and the samples were stored at 6 °C for 48 h. Afterwards, the samples were dehydrated with ethanol of low to high concentrations (30, 50, 70, 90, and 100%) and finally air dried. The samples were sputter coated with gold and observed with SEM at different magnifications.

Antibacterial evaluation

Antibacterial activity of *Artemisia annua* L. extract, PCL/gelatin and crosslinked PCL/gelatin–*Artemisia annua* L. against strain of *Staphylococcus aureus* as Gram-positive bacteria, was evaluated by disc diffusion method. This test was repeated three times for each identical sample. The top and bottom of electrospun samples were sterilized using UV light for 20 min prior to testing.

Disc diffusion tests were carried out using Mueller–Hinton Agar. Briefly, the agar surface was inoculated using a swab dipped in the bacterial cell suspension adjusted to a turbidity of 0.5 McFarland standard units and then allowed to dry for approximately 5 min. For *Artemisia annua* L. extract, 100 µL of 0.3 g of dissolved extract in 1 mL distilled water was incubated at 37 °C for 24 h after being placed in the culture medium.

The same procedure was used for the 1×1 cm^2 sterilized PCL/gelatin and crosslinked PCL/gelatin–*Artemisia annua* L. fibrous mats. It should be noted that Gentamicin discs (10 µg antibiotics) were used as a control sample. After 24 h, the antibacterial activity of the samples was evaluated by the measuring the diameter of the inhibition zone formed around the specimens.

Statistical analysis

The obtained data were reported as mean and standard deviation values. Data were analyzed by the Student *t* test with a significance of p values < 0.05. The SPSS software was carried out for statistical analysis (V 25, New York, USA).

Results and discussion

FTIR analysis

The FTIR spectrum (Fig. 2) of the *Artemisia annua* L. methanol extract revealed that it was composed of fatty acids, aromatic amines, aliphatic halo compounds, alkenes, alcohols, fluoro compounds, carboxylic acids, peroxides and cyclic compounds like cyclic ethers, etc. The related FTIR peak assignments for *Artemisia annua* L. are summarized in Table 1. The obtained results are in good agreement with other reported data (Harrigan and Goodacre 2003; Sharma et al. 2014; Hameed et al. 2016). Furthermore, ATR-FTIR analysis has been done to characterize the fabricated nanofibrous structures (Fig. 2). Existence of the characteristics peaks of *Artemisia annua* L. in the ATR-FTIR spectra of gelatin–*Artemisia annua* L. and PCL/gelatin–*Artemisia annua* L. electrospun nanofibrous samples confirms the successful electrospinning procedure for the fabrication of nanofibrous wound dressing containing *Artemisia annua* L. extract.

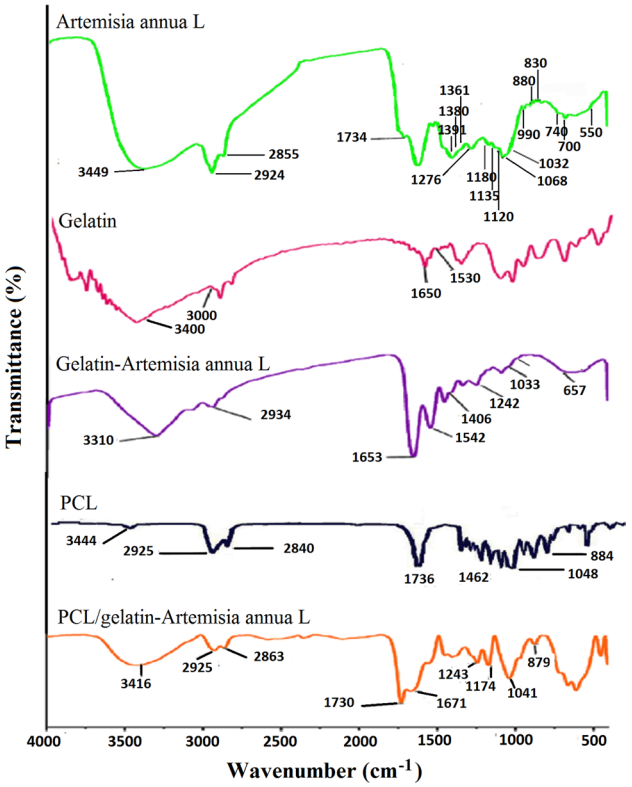

Fig. 2 FTIR spectra of *Artemisia annua* L. methanol extract together with ATR-FTIR spectra of the fabricated nanofibrous samples

Morphological properties of the fabricated wound dressing

Compared with the conventional rotating mandrel as collector that all of the spots can be possible sites for attracting the fibers, in the collector which is covered by the metal mesh, fibers are attracted by the metal walls and just

Table 1 FTIR peak assignments for *Artemisia annua* L. extract

No.	Frequency (cm^{-1})	Group of compounds	No.	Frequency (cm^{-1})	Group of compounds
1	3449	Aromatic primary amine compound	11	1135–1120	Alkyl substituted ether
2	3500–3200	Hydrogen-bonded alcohols, Phenols	12	1300–1050	Carboxylic acids
3	3000–2900	Fatty acids	13	1068	Cyclic ethers
4	2855	Methoxy	14	1032	Aliphatic fluoro compounds
5	1734	C=O stretching of the ester	15	990	Vinyl compounds
6	1460	Aromatic ring	16	880–830	Peroxides
7	1440	Methyl	17	675–995	Alkenes
8	1390–1360	Phenol	18	740–700	Aliphatic chloro compounds
9	1276	Primary or secondary alcohol	19	550	Aliphatic iodo compounds
10	1180	Tertiary amine			

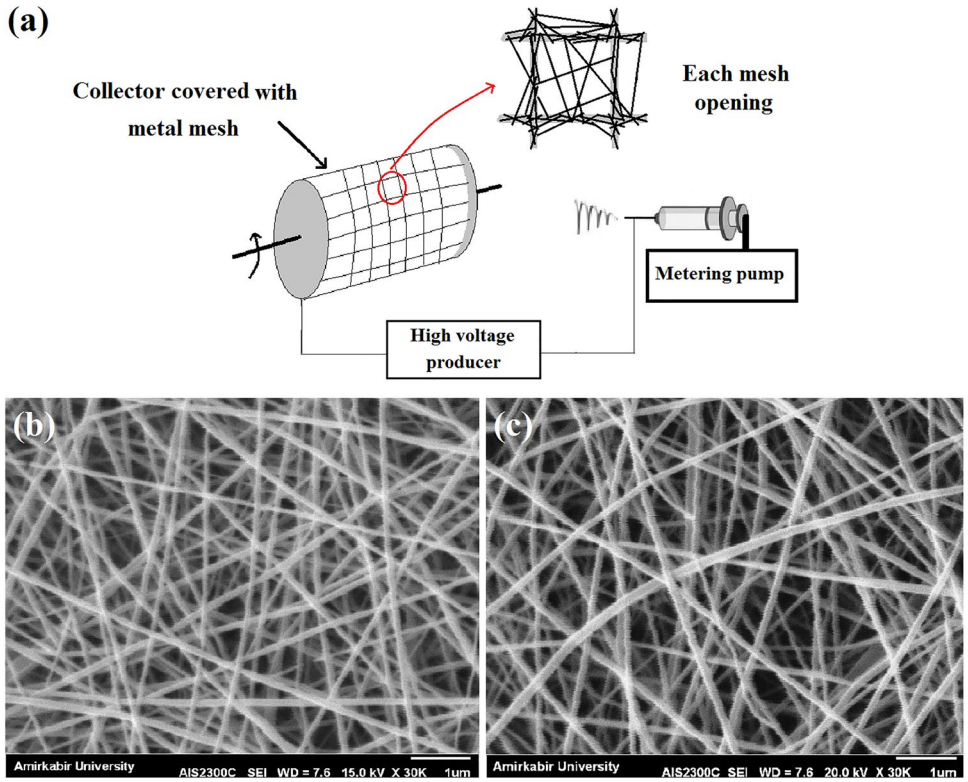

Fig. 3 **a** Schema of the setup used for the fabrication of wound dressings. In this schema, nanofiber collection manner on different regions of metal mesh (metal walls and mesh openings) is illustrated. **b** SEM image of the PCL nanofibers collected on the conventional rotating mandrel. **c** PCL nanofibers collected on the rotating mandrel covered with metal mesh

cross the non-conductive openings of the mesh (Fig. 3a). As such, accumulation of the fibers on the non-conductive regions (mesh openings) would be lower than other regions (schema of each mesh opening in Fig. 3a), and these regions can be the susceptible sites for oxygen permeability. SEM image of the PCL nanofibers collected on the conventional collector is presented in Fig. 3b. In addition, SEM image of the PCL nanofibers collected on the non-conductive regions of the collector which was covered by metal mesh is presented in Fig. 3c. According to these SEM images, lower compactness of nanofibers and the subsequent increased fiber-to-fiber distances can be seen for the PCL structure formed on non-conductive regions of the modified collector.

SEM images of the prepared nanofibrous structures (using the modified collector) together with the related fiber diameter distribution histograms are shown in Fig. 4. As can be seen, uniform nanofibers with average diameter of 124.00 ± 44.28 nm are formed by electrospinning the PCL solution (Fig. 4a, c). Furthermore, as can be seen in Fig. 4b, d, electrospinning of the gelatin–*Artemisia annua* L. blend was done successfully for the first time and results revealed the formation of nanofibers with an average diameter of about 242.00 ± 67.53 nm. Consequently, electrospinning of gelatin/*Artemisia annua* L. on top of PCL nanofibers produced the double-layer nanofibrous structure with proper microstructural properties for wound dressing application.

Artemisia annua L. extract release study

UV–Vis spectra of the *Artemisia annua* L. extract were obtained (Fig. 5a) and results revealed the characteristic peaks at 262, 288, 353–367 and 530–560 nm which corresponded to artemisinin component (Misra et al. 2013; Gafoori et al. 2013). These observation revealed the existence of artemisinin portion in the prepared methanol extract of *Artemisia annua* L. plant, which is the most valuable and important component of this plant possessing various properties such as antimicrobial, antibacterial, and anti-inflammatory properties. The above-mentioned peaks as well as other peaks of the *Artemisia annua* L. extract UV–Vis spectra at 470, 510 and 669–678 nm may correspond to the characteristic peaks of other component in the plant such as artemisinic acid, scopoletin, casticine, rosmarinic acid (Hasnaeni et al. 2017; Schmidt 2014; Anshul et al. 2013). Furthermore, the observed peaks in UV–Vis spectra of the *Artemisia annua* L extract may correspond to the natural pigments in this plant extract, specially the peaks in 480–510 nm range which can be correlated with green pigments.

The optical absorption of the prepared nanofibrous sample extracts in PBS was considered for the determination of *Artemisia annua* L. release over the time (Fig. 5b–e). UV–Vis absorbance peaks at 220 and 260–280 nm were observed in the spectrum of the samples which could relate to PCL/gelatin (PG) nanofibrous mats. The observed

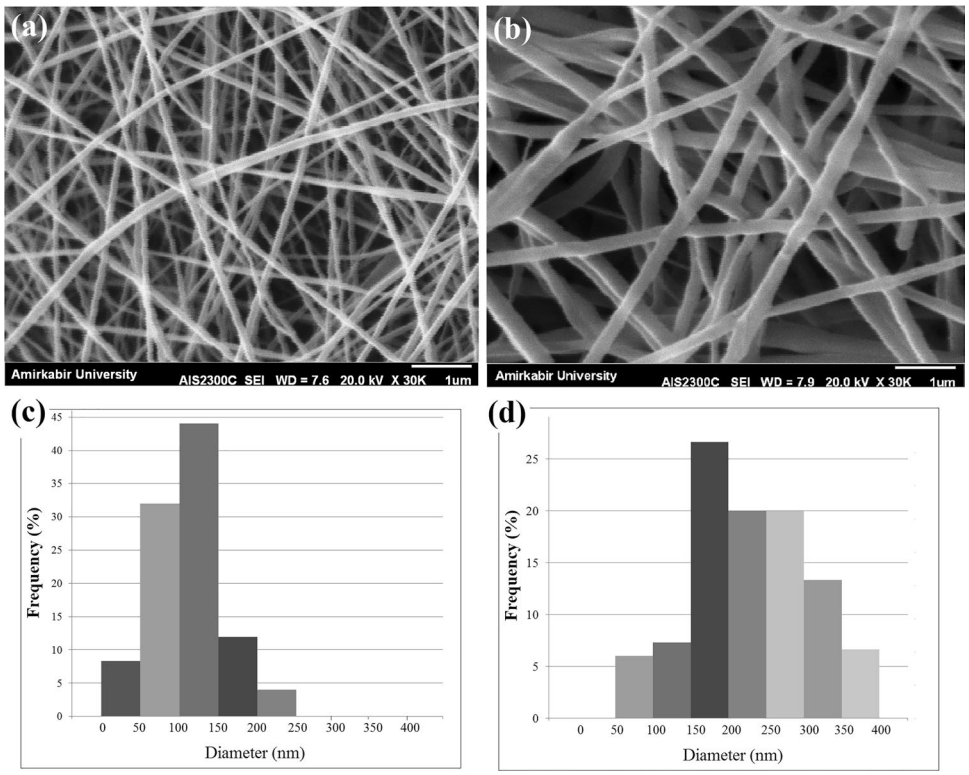

Fig. 4 SEM micrographs of the electrospun PCL (**a**), and gelatin/*Artemisia annua* L. (**b**) nanofibrous structures collected on the modified collector (rotating mandrel covered with the metal mesh), together with their fiber diameter distribution histograms [PCL (**c**), and gelatin/*Artemisia annua* L. (**d**)]

UV–Vis absorbance peaks were characteristic peaks of gelatin (Hermanto et al. 2013; Liu et al. 2011; Paul Das et al. 2017). On the other hand, the UV–Vis spectrum of the samples was related to PCL/gelatin–*Artemisia annua* L. nanofibrous mats (PGA and PGA-x). The absorbance peaks at wavelengths of 212 and 260–290 nm were considered as the overlap region of gelatin and *Artemisia annua* L. characteristics peaks. Furthermore, the absorbance peaks at wavelengths of 350, 460 and 670 nm which appeared in UV–Vis absorbance spectra of the samples were related to PGA and PGA-x, as the characteristic peaks of *Artemisia annua* L. extract that were detected in the UV–Vis absorbance spectrum of this plant extract.

In comparison between the *Artemisia annua* L. containing and non-containing samples in overlap region, mild shifts in the peak existed in 212–228 nm as well as the peak observed in the range of 260–290 to 270–300 nm. In addition, the crosslinked samples revealed the lower peak intensities after the 1 and 3 days but higher peak intensities after 5 and 7 days compared to the samples without crosslinking. The obtained results confirmed the sustained release of the plant extract over the experiment time in the crosslinked PCL/gelatin–*Artemisia annua* L. sample.

To evaluate the *Artemisia annua* L. extract release quantitatively, wavelength of 350 nm was considered to observe the absorbance. Wavelength of 350 nm was chosen because one of the important characteristic peaks of the extract which is related to the artemisinin component appears in this wavelength. Furthermore, at this wavelength, there is no compliance of absorption peaks of the other releasing component, gelatin, with *Artemisia annua* L. absorbance peak. For this aim, standard solutions of *Artemisia annua* L. were prepared (0.1–1.0 mg/mL) and calibration curve was drawn by absorbance intensity (at 350 nm) of each solution with certain concentration. In the given concentration range, linear region in the calibration curve with adsorption intensities less than 1 was obtained. The amount of the plant extract in the incubating solutions containing the fabricated wound dressings at different time points was calculated by comparing the intensity of the UV–Vis absorbance (at 350 nm) of these solution samples with those of standard solutions using the drawn calibration curve, and extending the value to the total volume of incubating medium. The percentage of *Artemisia annua* L. extract released from the fabricated wound dressing samples over the time was obtained by dividing the calculated amount of the plant extract in the incubating solutions to the initial amount of plant extract in these samples. The initial amount of the plant extract was calculated by accurate weighing of each sample before incubation and multiplying the obtained weight by the extract weight ratio that was considered in the fabrication step. Figure 5f illustrates the percentage of *Artemisia annua* L. extract in vitro release from the fabricated wound dressing samples over 7 days. As can be seen, the plant extract was released rapidly from PGA sample at the first day of incubation following by the slight increase in the subsequent time points. While for

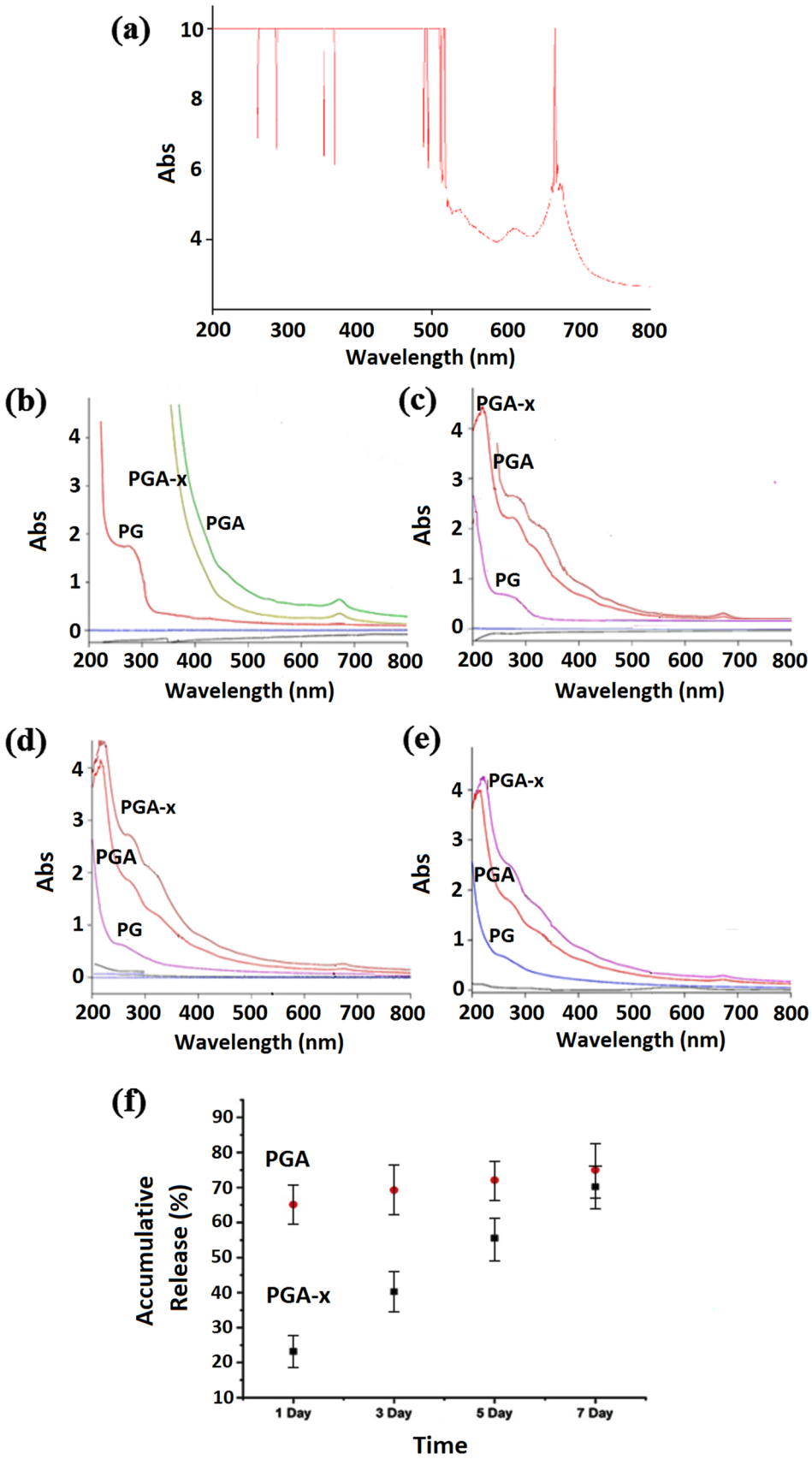

Fig. 5 **a** UV–Vis absorption spectra of *Artemisia annua* L. extract. **b–e** UV–Vis absorption spectra of PBS solutions containing PCL/gelatin (PG), PCL/gelatin–*Artemisia annua* L. extract (PGA) and crosslinked PCL/gelatin–*Artemisia annua* L. extract (PGA-x) samples at 1st, 3rd, 5th and 7th day of incubation, respectively. **f** Accumulative release of *Artemisia annua* L. from PCL/gelatin–*Artemisia annua* L. (PGA) and crosslinked PCL/gelatin–*Artemisia annua* L. (PGA-x) samples after 1st, 3rd, 5th and 7th days of incubation by analyzing absorbance at 350 nm

the crosslinked sample (PGA-x), a sustained release over the experiment period was observed which confirmed the success in the fabrication technique of wound dressing containing the *Artemisia annua* L. extract. The release test period through the fabricated wound dressing is a combination of bulk diffusion (because of high hydrophilicity of gelatin) and degradation mechanisms (because of the degradable nature of the applied materials). By the way, intensity and contribution of the mentioned mechanisms would be varied based on the degree of crosslinking (Torres-Martínez et al. 2018; Munj et al. 2016; Laha et al. 2017; Goonoo et al. 2014).

Morphological stability

To examine the morphological stability of the prepared structures in biological condition, the prepared samples were put in PBS solution for 1 and 3 days and after vacuum drying, SEM images were taken from their surfaces (Fig. 6). As can be seen, crosslinked PCL/gelatin–*Artemisia annua* L. nanofibrous structure presents a good structural stability over the test period (e, f) compared with PCL/gelatin (a, b) and un-crosslinked PCL/gelatin–*Artemisia annua* L. (c, d) samples. These observations are consistent with the results of the release study which indicates a gradual degradation of nanofibers and subsequent sustain release of the plant extract from the crosslinked PCL/gelatin–*Artemisia annua* L. wound dressing.

Mechanical properties

Mechanical properties of wound dressings are important parameters which indicate the applicability of the structure

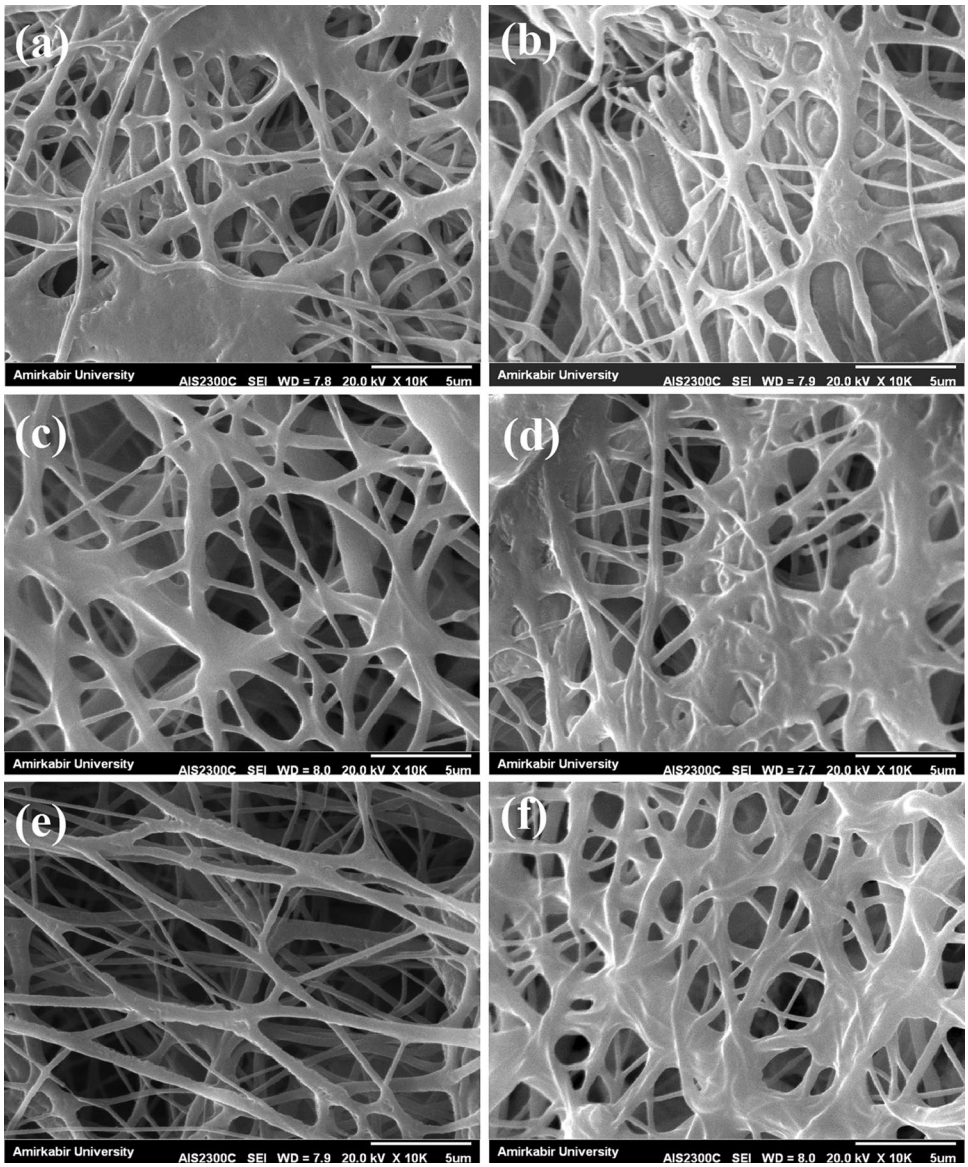

Fig. 6 SEM images from the surface of PCL/gelatin (PG) (**a**, **b**), PCL/gelatin–*Artemisia annua* L. (PGA) (**c**, **d**), and crosslinked PCL/gelatin–*Artemisia annua* L. (PGA-x) (**e**, **f**) samples after 1 and 3 days of immersion in PBS solution

to be used in a certain condition. In skin sites, especially where the tissue is at the exposure of frequent tensile stresses, tensile modulus as well as tensile strength and elongation-at-break are important factors for a wound dressing to perform well. In this study, tensile test was applied on the fabricated samples and the obtained results are reported in Table 2. The fabricated wound dressings in the present work revealed the proper and acceptable mechanical properties compared with other reported wound dressings in the literature. According to the reported data in Table 2, mechanical properties of the crosslinked samples are to some extent lower than those of uncrosslinked samples. By the way, crosslinked PCL/gelatin–*Artemisia annua* L. samples possess the required mechanical properties to be used as wound dressing. In fact the intensity and duration of crosslinking procedure (being exposed to the vapor of diluted glutaraldehyde solution (2.5%) just for 5 h) was set so that an acceptable sustain release and moderate stability would be obtained without a serious destruction of mechanical strength.

In vitro cytotoxicity and cell proliferation evaluation

Quantitative in vitro cytocompatibility results of the prepared wound dressing samples evaluated by MTT test are reported in Fig. 7. At the early time points (day 1 and 4), significant differences ($p < 0.05$) were observed comparing the cell viability on the control (i.e., TCPS) to that on the prepared samples. Increasing the culture time, no significant difference ($p > 0.05$) was observed between TCPS and the fabricated structure, indicating an increased cell activity and cell proliferation rate on the fabricated structures rather than on TCPS. On the other hand, despite the sustain release of *Artemisia annua* L. from the prepared sample in the cell culture media (which was observed in release study), no cytotoxicity and no inhibition towards cellular proliferation was observed. In addition, there was no significant difference between the results of PCL/gelatin and crosslinked PCL/gelatin–*Artemisia annua* L. samples indicating the proper biological properties of *Artemisia annua* L. extract.

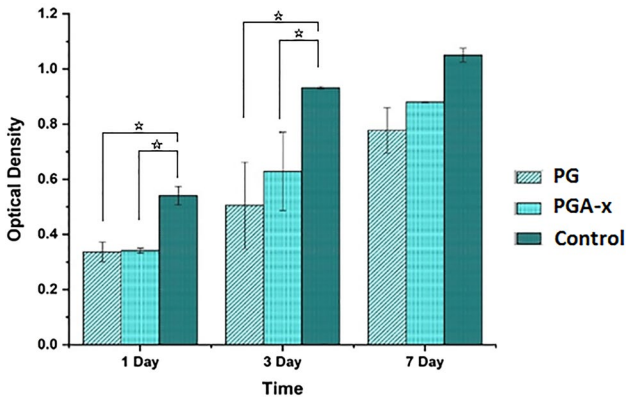

Fig. 7 Survey of viability and proliferation of L929 fibroblast cells on the PCL/gelatin and crosslinked PCL/gelatin–*Artemisia annua* L. samples compared to the TCPs as control, at 1st, 3rd and 7th days of culture. Statistically significant difference is denoted as *($p < 0.05$)

Cell morphological observation

L929 fibroblast cells were seeded onto the prepared electrospun structures and SEM observation was performed to investigate cell attachment and morphology of the samples. Cell seeding was done on the surface of gelatin and gelatin/*Artemisia annua* L. nanofibrous side of PCL/gelatin and PCL/gelatin–*Artemisia annua* L. samples. SEM images of fibroblast cells seeded on the prepared electrospun mats are reported in Fig. 8. One day after seeding, good attachment of cells was observed on both PCL/gelatin and PCL/gelatin–*Artemisia annua* L. samples (Fig. 8a, c). Three days after cell seeding, considerable spreading of cells was observed on the surface of the both PCL/gelatin and PCL/gelatin–*Artemisia annua* L. samples (Fig. 8b,d). Results indicated that the presence of *Artemisia annua* L. extract had no adverse effect on cell attachment and spreading and the seeded cells could undergo their normal activities. These observations confirmed the proper biological properties of *Artemisia annua* L. extract which is comparable to the excellent properties of gelatin. The above results of cell attachment and spreading on the surface of the prepared wound

Table 2 Tensile mechanical properties of the PCL/gelatin–*Artemisia annua* L. (PGA) and crosslinked PCL/gelatin–*Artemisia annua* L. (PGA-x) samples

Mechanical property	Tensile modulus (MPa)	Tensile strength (MPa)	Elongation-at-break (%)
Sample			
PCL/gelatin–*Artemisia annua* L. nanofibrous mat before crosslinking (PGA)	122.00 ± 12.20 MPa	13.30 ± 2.58	47.70 ± 5.12
Crosslinked PCL/gelatin–*Artemisia annua* L. nanofibrous mat (PGA-X)	108.00 ± 14.60 MPa	10.60 ± 3.37	34.40 ± 3.76

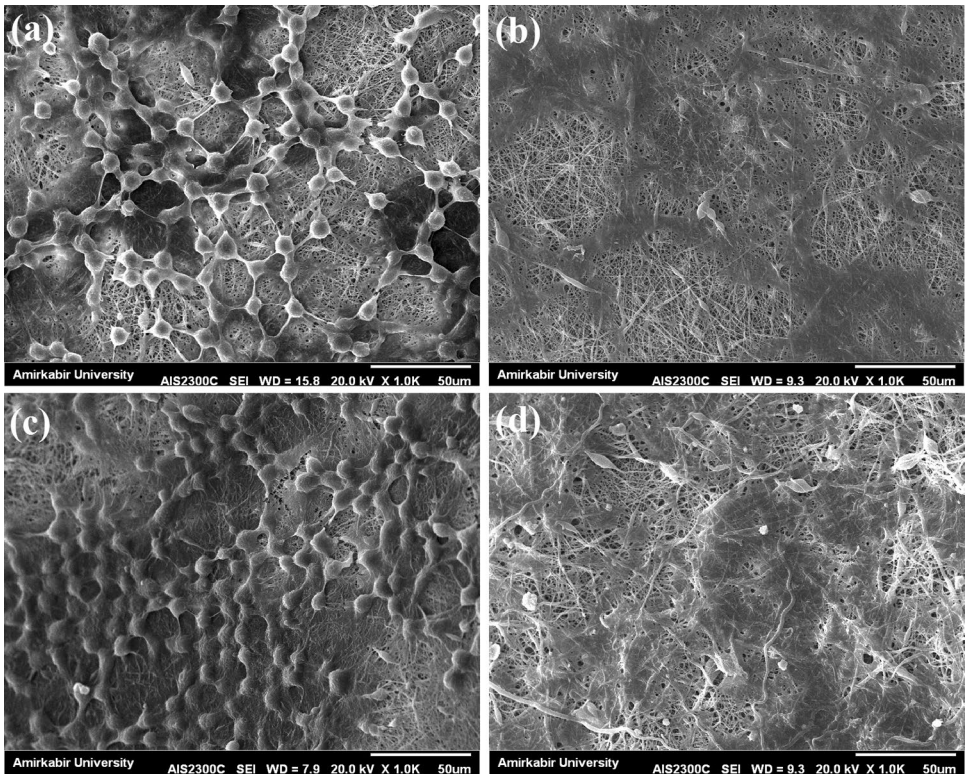

Fig. 8 SEM images of the fibroblast cells morphology on the **a** PCL/gelatin (PG), one day after cell culture, **b** PCL/gelatin (PG), 3 days after cell culture, **c** crosslinked PCL/gelatin–*Artemisia annua* L. (PGA-x), 1 day after cell culture, **d** crosslinked PCL/gelatin–*Artemisia annua* L. (PGA-x), 3 days after cell culture

dressing samples are in a good agreement with the obtained results from the cell proliferation test.

Antibacterial evaluation

The antibacterial property of wound dressings plays a crucial role in their application. In this study, the antibacterial activity of PCL/gelatin (PG) and crosslinked PCL/gelatin–*Artemisia annua* L. (PGA-x) nanofibrous samples were tested against *Staphylococcus aureus* by disc diffusion method. According to the results (Fig. 9), no antibacterial activity was detected for PCL/gelatin (PG), but PCL/gelatin–*Artemisia annua* L. (PGA-x) nanofibrous samples exhibited antibacterial activity against *Staphylococcus aureus*. Although the clarity of inhibition zone was reduced due to the diffusion of green-color pigments from the plant extract to the agar medium, the bacterial growth inhibition region can be distinguished according to the difference in color of each region. The zone of inhibition related to the samples containing the *Artemisia annua* L. extract (PGA-x) was measured as 5.00 ± 0.20 mm, while for the sample without the plant extract (PG) no zone of inhibition was found. It has been

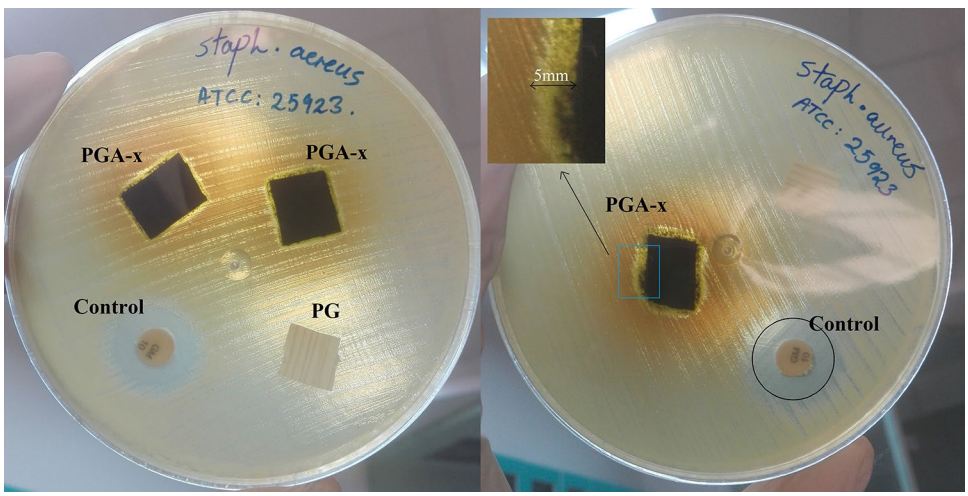

Fig. 9 Antibacterial activity of PCL/gelatin as well as PCL/gelatin–*Artemisia annua* L. nanofibrous wound dressing samples against *Staphylococcus aureus* bacteria. Gentamicin discs (10 µg antibiotics) were used as a control. Samples names are shown beside each one

reported that the main component in *Artemisia annua* L., artemisinin, contains a peroxide bridge and is known to have antibacterial activity (Kim et al. 2015).

Conclusion

In this study, the *Artemisia annua* L. was extracted as herbal drug and utilized for the first time in the composition of polymeric wound dressing. Gelatin–*Artemisia annua* L. nanofibers with average fiber diameter of 242.00 ± 67.53 nm were prepared for the first time using electrospinning method. Subsequently, double-layer nanofibrous PCL/gelatin–*Artemisia annua* L. (PGA) and crosslinked-PCL/gelatin–*Artemisia annua* L. (PGA-x) samples were fabricated. The prepared PGA-x wound dressing with desirable physical and mechanical properties (tensile modulus of 108.00 ± 14.60) encouraged the attachment, spreading and proliferation of the fibroblast cells with potent antibacterial properties against *Staphylococcus aureus* (inhibition zone of 5.00 ± 0.20 mm). The fast release of extract from the electrospun PCL/gelatin–*Artemisia annua* L. mat was effectively overcome by crosslinking the prepared structure and consequently a novel *Artemisia annua* L.-containing wound dressing possessing a sustain release of the plant extract (over 7 days) was produced. The degradation study inferred that the fabricated wound dressing was structurally stable in biological condition during 3 days, thereby reducing the frequency of dressings during the wound healing process. In conclusion, the prepared crosslinked-PCL/gelatin–*Artemisia annua* L. sample has a potential to be used as nanofibrous antibacterial wound dressing in near future.

Compliance with ethical standards

Conflict of interest The authors declare that they have no conflict of interest.

Ethical approval This article does not contain any studies with human participants or animals.

References

Anke H, Sterner O (1991) Comparison of the antimicrobial and cytotoxic activities of twenty unsaturated sesquiterpene dialdehydes from plants and mushrooms. Planta Med 57:344–346. https://doi.org/10.1055/s-2006-960114

Anshul N, Bhakuni RS, Gaur R, Singh D (2013) Isomeric flavonoids of *Artemisia annua*(Asterales: Asteraceae) as insect growth inhibitors against *Helicoverpa armigera* (Lepidoptera: Noctuidae) Florida. Entomologist 96:897–903

Belachew TF, Asrade S, Geta M, Fentahun E (2020) In vivo evaluation of wound healing and anti-inflammatory activity of 80% methanol crude flower extract of *Hagenia abyssinica* (Bruce) J.F. Gmel in mice. Evid Based Complement Altern Med. https://doi.org/10.1155/2020/9645792

Bhakuni RS, Jain DC, Sharma RP, Kumar S (2001) Secondary metabolites of *Artemisia annua* and their biological activity. Curr Sci India 80:35–48

Böttcher-Haberzeth S, Biedermann T, Reichmann E (2010) Tissue engineering of skin. Burns. 36(4):450–460

Brown GD (2010) The biosynthesis of artemisinin (Qinghaosu) and the phytochemistry of *Artemisia annua* L. (Qinghao). Molecules 15:7603–7698. https://doi.org/10.3390/molecules15117603

Cavar S, Maksimovi´ca M, Vidica D, Pari´cb A, (2012) Chemical composition and antioxidant and antimicrobial activity of essential oil of *Artemisia annua* L. from Bosnia. Ind Crops Prod 37:479–485

Czechowski T, LarsonTR CataniaTM, Harvey D, Wei C, EssomeM BGD, Graham IA (2018) Detailed phytochemical analysis of high- and low artemisinin-producing chemotypes of *Artemisia annua*. Front Plant Sci 9:641

De Vries PJ, Dien TK (1996) Clinical pharmacology and therapeutic potential of artemisinin and its derivatives in the treatment of malaria. Drugs 52:818–836

Derda M, Hadaś E, Cholewiński M, Skrzypczak L, Grzondziel A, Wojtkowiak-Giera A (2016) *Artemisia annua* L. as a plant with potential use in the treatment of acanthamoebiasis. Parasitol Res 115:1635–1639

Donata R, Santomauro F, Bilia AR, Flamini G, Sacca C (2015) Antibacterial activity of Tuscan *Artemisia annua* essential oil and its major components against some foodborne pathogens. LWT Food Sci Technol 64:1251–1254

Gafoori H, Sariri R, Naghavi MR, Aryakia E, Dolatyari A, Shahzadeh Fazli SA, Ramazani H, Farahmand (2013) Analysis of artemisinin isolated from *Artemisia annua* L. by TLC and HPLC. J Liq Chromat Relat Technol 36:1198–1206

Goonoo N, Bhaw-Luximon A, Jhurry D (2014) Drug loading and release from electrospun biodegradable nanofibers. J Biomed Nanotechnol 10:2173–2199

Hameed IH, Altameme HJ, Idan SA (2016) *Artemisia annua*: biochemical products analysis of methanolic aerial parts extract and anti-microbial capacity. Res J Pharm Biol Chem Sci 7:1843–1867

Harrigan GG, Goodacre R (2003) Metabolic profiling: its role in biomarker discovery and gene function analysis. Kluwer Academic, Boston, pp 293–309

Hasnaeni H, Sudarsono S, Nurrochmad A, Widyarini S (2017) Identification of active anti-inflammatory principles of betabeta wood (*Lunasia amara* Blanco) from Siawung Barru-South Sulawesi, Indonesia. Trop J Pharm Res 16(1):161

Hejazi F, Mirzadeh H (2016) Roll-designed 3D nanofibrous scaffold suitable for regeneration of load bearing bone defects. J Prog Biomat 5:199–201

Hermanto S, Sumarlin LO, Fatimah W (2013) Differentiation of bovine and porcine gelatin based on spectroscopic and electrophoretic analysis. J Food Pharm Sci 68–73

Hien TT, White NJ (1993) Qinghaosu. Lancet 341:603–608

Kaboutari Katadj J, Rafieian-Kopaei M, Nourani H, Karimi B (2016) Wound healing effects of *Artemisia sieberi* extract on the second degree burn in mice skin. J HerbMed Pharmacol 5:67–71

Kim WS, Chio WJ, Lee S, Kim WJ, Lee DC, Sohn UD, Shin HS, Kim W (2015) Anti-inflammatory, antioxidant and antimicrobial effects of Artemisinin extracts from *Artemisia annua* L. Korean J Physiol Pharmacol 19:21–27

Krishnan KA, Thomas S (2019) Recent advances on herb-derived constituents-incorporated wound-dressing materials: a review. Polym Adv Technol 30:823–838

Laha A, Sharma CS, Majumdar S (2017) Sustained drug release from multi-layered sequentially crosslinked electrospun

gelatin nanofiber mesh. Mater Sci Eng C. https://doi.org/10.1016/j.msec.2017.03.110
Liu X, Jia G (2018) Modern wound dressing using polymers/biopolymers. J Mater Sci Eng 7:3
Liu Y, Liu X, Wang X (2011) Biomimetic synthesis of gelatin polypeptide-assisted nobel-metal nanoparticles and their interaction study. Nanoscale Res Lett 6:22
Misra H, Mehta D, Mehta BK, Jain DC (2013) Microwave-assisted extraction studies of target analyte artemisinin from dried leaves of *Artemisia annua* L. Org Chem Int 2013:1–6
Munj HR, Lannutti JJ, Tomasko DL (2016) Understanding drug release from PCL/gelatin electrospun blends. J Biomat Appl. https://doi.org/10.1177/0885328216673555
Naseri-Nosar M, Ziora ZM (2018) Wound dressing from naturally-occurring polymers: a review on homo polysaccharide-based composites. Carbohydr Polym 189:379–398
Nguyen DT, Göpfert JC, Ikezawa N, MacNevin G, Kathiresan M, Conrad J, Spring O, Ro DK (2010) Biochemical conservation and evolution of germacrene a oxidase in Asteraceae. J Biol Chem 285(22):16588–16598
Niu X, Xing W, Li W, Fan T, Hu H, Li Y (2012) Isofraxidin exhibited anti-inflammatory effects in vivo and inhibited TNF-alpha production in LPS induced mouse peritoneal macrophages in vitro via the MAPK pathway. Int Immunopharmacol 14:164–171. https://doi.org/10.1016/j.intimp.2012.06.022
Okur ME, Karantas ID, Senyigit Z, Okur NU, Siafaka PI (2020) Recent trends on wound management: new therapeutic choices based on polymeric carriers. Asian J Pharm Sci. https://doi.org/10.1016/j.ajps.2019.11.008
Paul Das M, Suguna PR, Prasad K, Vijayakshmi JV, RenukaM. (2017) Extraction and characterization of gelatin: a functional biopolymer. Int J Pharm Pharm Sci 9:239–242
Ranjbar R, Yousefi A (2018) *Artemisia dracunculus* in combination with chitosan nanoparticle biofilm improves wound healing in MRSA infected excisional wounds: an animal model study. Eur Asia J Biosci 12:219–226
Rezvani Ghomi E, Khalili SH, Nouri Khorasani S, Esmaeely Neisiany R, Ramakrishna S (2019) Wound dressings: current advances and future directions. J Appl Polym Sci 136(27):47738
Santomauro F, Donato R, Sacco C, Pini G, Flamini G, Bilia AR (2016) Vapour and liquid-phase *Artemisia annua* essential oil activities against several clinical strains of candida. Planta Med 82:1016–1020. https://doi.org/10.1055/s-0042-108740
Schmidt H, Günther C, Weber M, Spörlein C, Loscher S, Bötcher C, Schobert R, Clemens S (2014) Metabolome analysis of *Arabidopsis thaliana* roots identifies a key metabolic pathway for iron acquisition. PLoS ONE 9(7):e102444
Sharma G, Kapoor H, Chopra M, Kumar K, Agrawal V (2014) Strong larvicidal potential of *Artemisia annua* leaf extract against malaria (*Anopheles stephensi* Liston) and dengue (*Aedes aegypti* L.) vectors and bioassay-driven isolation of the marker compounds. Parasitol Res 113:197–209
Singer AJ, Clark RAFN (1999) Mechanisms of disease: cutaneous wound healing. Engl J Med 341(10):738–746
Stoica AE, Chircov C, Grumezescu AM (2020) Nanomaterials for wound dressings: an up-to-date overview. Molecules 25:2699. https://doi.org/10.3390/molecules25112699
Torres-Martínez EJ, Cornejo Bravo JM, Medina AS, Pérez González GL, Villarreal Gómez LZ (2018) A summary of electrospun nanofibers as drug delivery system: drugs loaded and biopolymers used as matrices. Curr Drug Deliv 15:1360–1374
Verdian-rizi MR, Sadat-Ebrahimi E, Hadjiakhoondi A, Fazeli, Pirali Hamedani M (2008) Chemical composition and antimicrobial activity of *Artemisia annua* L. essential oil from Iran. J Med Plant 7:58–62
Yamazaki T, Tokiwa T (2010) Isofraxidin, a coumarin component from *Acanthopanax senticosus*, inhibits matrix metalloproteinase-7 expression and cell invasion of human hepatoma cells. Biol Pharm Bull 33:1716–1722. https://doi.org/10.1248/bpb.33.1716